

Article

Preparation of Magnetic Molecularly Imprinted Polymer for Methylene Blue Capture

Anastasia Sedelnikova, Yuliya Poletaeva, Victor Golyshev , Alexey Chubarov *  and Elena Dmitrienko * 

Institute of Chemical Biology and Fundamental Medicine SB RAS, 630090 Novosibirsk, Russia

* Correspondence: chubarov@niboch.nsc.ru or chubarovalesha@mail.ru (A.C.); elenad@niboch.nsc.ru (E.D.);
Tel.: +7-913-763-1420 (A.C.); +7-913-904-1742 (E.D.)

Abstract: Hybrid magnetic molecularly imprinted polymers (MMIPs) have the advantages of the technology of molecularly imprinted material and magnetic nanoparticles. The magnetic properties of MMIPs allow easy magnetic separation of various pollutants and analytes. A convenient and simple approach has been developed for the preparation of MMIPs based on polyamide (nylon-6) and magnetic nanoparticles. The polymer matrix was formed during the transition of nylon-6 from a dissolved state to a solid state in the presence of template molecules and Fe₃O₄ nanoparticles in the initial solution. Methylene blue (MB) was used as a model imprinted template molecule. The MMIPs exhibited a maximum adsorption amount of MB reached 110 μmol/g. The selectivity coefficients toward MB structural analogs were estimated to be 6.1 ± 0.6 and 2.1 ± 0.3 for 15 μM hydroxyethylphenazine and toluidine blue, which shows high MMIP selectivity. To prove the MMIPs' specificity in MB recognition, magnetic nonimprinted polymers (MNIPs) were synthesized without the presence of a template molecule. MMIPs exhibited much higher specificity in comparison to MNIPs. To show the remarkable reusability of the MMIP sorbent, more than four MB absorption and release cycles were carried out, demonstrating almost the same extraction capacity step by step. We believe that the proposed molecular imprinting technology, shown in the MB magnetic separation example, will bring new advances in the area of MMIPs for various applications.

Keywords: methylene blue; methylene blue capture; molecularly imprinted polymer; magnetic molecularly imprinted polymer; magnetic molecularly imprinted solid-phase extraction; magnetic solid-phase microextraction; specific recognition; nylon-6; reusability



Citation: Sedelnikova, A.; Poletaeva, Y.; Golyshev, V.; Chubarov, A.; Dmitrienko, E. Preparation of Magnetic Molecularly Imprinted Polymer for Methylene Blue Capture. *Magnetochemistry* **2023**, *9*, 196. <https://doi.org/10.3390/magnetochemistry9080196>

Academic Editor: Evgeny Katz

Received: 30 June 2023

Revised: 19 July 2023

Accepted: 28 July 2023

Published: 31 July 2023



Copyright: © 2023 by the authors. Licensee MDPI, Basel, Switzerland. This article is an open access article distributed under the terms and conditions of the Creative Commons Attribution (CC BY) license (<https://creativecommons.org/licenses/by/4.0/>).

1. Introduction

Methylene blue (MB) is a cationic thiazine dye widely used as a model target for magnetic separation or sensing applications of sorbents [1–6]. Due to its photochemical properties, MB inactivates multidrug-resistant bacteria and may be used for cancer treatment [1,4]. On the other hand, MB is an important industry dye and, therefore, a prevalent pollutant, which is toxic in high concentrations [1–3]. In these contexts, MB may be used for therapeutic applications or should be detected and measured or removed from the water for safety [1–4]. Herein, MB was chosen as a template molecule for molecular imprinting performance.

Molecular imprinting is a unique technique for creating template-shaped cavities in polymer matrices with predetermined high specificity [7–11]. The approach resembles an enzyme–substrate “lock and key” model. Polymers with template-specific cavities are called molecularly imprinted polymers (MIPs) [9,10]. MIPs are typically synthesized in a three-step process. The functional monomers interact with the template molecule (Figure 1A). After that, the cross-linker or polymerization initiator is added, forming a polymer with template-bounded cavities. Finally, the template molecule is removed, resulting in a cross-linked material with high-affinity cavities for the target compound [7–10,12–14]. The combination of MIP recognition and magnetic nanoparticles in one system results in

a novel material, also known as magnetic MIPs (MMIPs) [7,12]. Manipulation with an external magnetic field opens the possibility of unique applications for MMIPs, which may be used for solid-phase extraction of pollutants in water samples (pesticides, herbicides, antibiotics, dyes, heavy metals, etc.) [7,8,12,15–24], photocatalytic and dark-condition degradation of pollutants [23], isolating active compounds contained in plants (alkaloids, flavonoids, terpenes, etc.) [12], enantioseparation [25], and the separation, purification, and detection of various biomolecules [22,26–28]. MMIPs show excellent selective binding to target compounds and can be quickly separated and easily removed from samples using an external magnet, thus avoiding time-consuming and tedious steps (centrifugation or filtration) [7,8,12,18–21,25–28]. The ability to adsorb and desorb analytes on a magnetic sorbent provides specific extraction, purification, and enrichment of the target compounds [28–30]. Furthermore, several emerging techniques (biosensor, chemiluminescence, etc.) based on MMIPs also offer new insights into pesticides [22], mycotoxins [22], antibiotics and drugs [18,20,22], protein [26], DNA and RNA [27], antibodies [22,26], and cancer biomarker [31] detection. Recently, MMIPs have begun to be used in various fields of biomedicine, such as disease diagnosis [31,32], pH and reducing stimuli-responsive drug and gene delivery [32–35], tumor imaging [33,34], and theranostics [33,34,36].

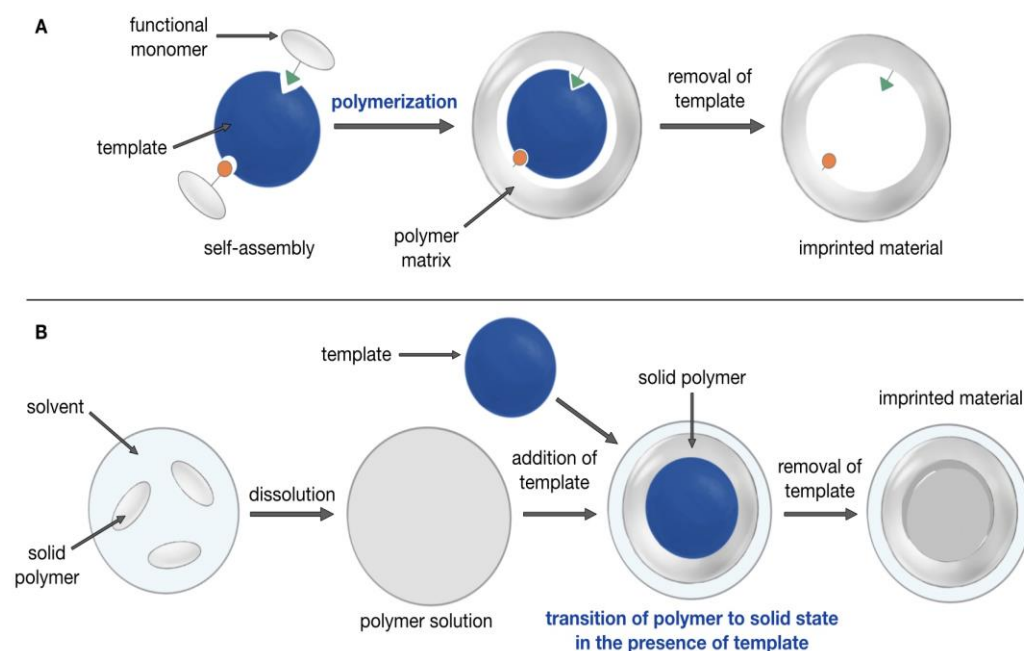


Figure 1. Schematic representation of the primary molecular imprinting process (A) and that in the present paper (B).

An alternative to the primary MIP synthesis by polymerization presented in Figure 1A may be a procedure involving off-the-shelf polymers (Figure 1B) [10,37]. The main idea of the imprinting consists of the two steps of one-pot synthesis. A polymer is dissolved in an organic solvent to give the specific interaction between the polymer chains and template in the solution. After precipitation or drying of the solution, the template is removed (Figure 1). Such a MIP is synthesized upon the transition of the polymer from a solute to a solid state and structural changes of the template. The advantages of the methods include an absence of functional monomers or cross-linking agents, a polymerization step, and easy and cheap synthesis [10]. The obtained cavities in MIPs specifically interact with template molecules, yielding a high-affinity complex.

The organic polymer matrices of MIPs allow for great diversification of their properties, such as thermal, chemical, or colloidal stability; charge; functional groups; etc. [7,9,10,12]. One of the polymers with distinct physical, chemical, and biological properties is nylon-6 [38–41]. Nylon provides high physical and chemical stability and low toxicity, which allows this

biocompatible polymer to be used for manufacturing various medical tools [38–41]. Highly soluble in organic solvents, the polyamide polymer nylon can be re-precipitated and reformed easily, forming various types of porous structures [38,39,42,43], which in this work will be used for the first time for MMIPs synthesis. The introduction of ferrimagnetic magnetite nanoparticles (Fe_3O_4 , MNPs) [33,34,36,44] into the nylon solution makes it possible to form MIPs on the surface of the nanoparticles, imparting magnetic properties to them. Nowadays, coated MNPs find vast applications in nanomedicine, magnetic separation, imaging, and theranostics [28,29,45–49]. Previously [39,43], we have shown the possibility of nylon coating on MNPs for nucleic acid microextraction and therapeutic applications. The proposed approach makes it possible to design polymer matrices for various tasks; for example, sensing surfaces or microparticle sorbents.

This work aimed to develop a simple, cost-effective, and convenient approach for MMIP synthesis using off-the-shelf polymer technology. The nylon-6 polyamide polymer and magnetite nanoparticles were used as a matrix and magnetic core, respectively, for MMIP manufacturing. To show proof of the concept of molecular imprinting technology and MMIP synthesis, the magnetic separation of MB was chosen. It should be noted that MB was used mostly as a model template molecule, which allows us to test the capacity, selectivity, and specificity of MMIPs. The employed imprinting method may also be extended to various applications and other templates, which have poor functionality for the usual pre-polymerization complex formation. Finally, MMIPs prepared using our imprinting technique can solve problems, such as a low abundance of functional monomer and cross-linker for the superfine structure of MIP, more types of cores to be exploited for coating with MIP shells, etc., associated with MIPs prepared by polymerization methods [50].

2. Materials and Methods

2.1. Materials

The $\text{FeCl}_3 \cdot 6\text{H}_2\text{O}$ was purchased from PanReac AppliChem (MW = 270.32, 97–102%). The $\text{FeCl}_2 \cdot 4\text{H}_2\text{O}$ was obtained from Acros organics (MW = 198.81, 99+%). 2,2,2-Trifluoroethanol (TFE) was acquired from Panreac Química (Barcelona, Spain). Nylon 6 (Product No. 181110), toluidine blue (TB), and hydroxyethylphenazine (PH) were purchased from Sigma (St. Louis, MO, USA) at the highest available grade and used without purification. The molecular weight (M_{wv}) of nylon 6 was measured as 22.5 ± 1 kDa by viscosimetry. All solutions were prepared using milliQ water ($18.2 \text{ M}\Omega\text{cm}$).

2.2. Synthesis of Magnetic Nanoparticles (MNPs)

The magnetic nanoparticles (MNPs) were synthesized according to the previously published method [39,51,52]. For the production, deoxygenated aqueous solutions of $\text{Fe}^{2+}/\text{Fe}^{3+}$ salts in a ratio of 1:2 without any stabilized agents were used. The MNP precipitation was carried out in an aqueous ammonia solution under stirring (500 rpm), and an argon atmosphere at 20 °C. The resulting MNPs had an average size of 11.0 ± 2.0 nm as determined by TEM.

2.3. Synthesis of MMIPs

Nylon-6 was dissolved in TFE to obtain a 5% solution. Aliquots of three different volumes were taken from the suspension of MNPs in water, from which the supernatants were taken to obtain a precipitate of nanoparticles weighing 0.5, 2, or 5 mg. To the dry MNPs, 0.4 mL of water and 0.1 mL of methylene blue solution with a concentration of 1 mg/mL were added. The nylon-6 solution (1 mL) and nanoparticle suspension with template molecules were mixed on a submersible vertical stirrer. The reaction mixture was stirred (1400 rpm) at 25 °C for 24 h. Afterward, MMIPs were magnetically separated and washed with water. To extract the template molecules from the polymer structure, MMIPs were incubated with an aqueous solution containing 5% glacial acetic acid and 5% sodium dodecyl sulfate (SDS) under stirring (1400 rpm) at 60 °C for 1 h. MMIPs were magnetically separated and washed with water.

The MMIP samples were named MMIP_0.5, MMIP_2, and MMIP_5, which represent the initial amount of MNPs of 0.5, 2, or 5 mg for the synthesis.

2.4. Synthesis of MNIPs

Magnetic nonimprinted polymers (MNIPs) were synthesized by the same procedure as for MMIPs (Section 2.3). However, no template molecule was used. The MNIPs were washed with an aqueous solution containing 5% glacial acetic acid and 5% SDS under stirring (1400 rpm) at 60 °C for 1 h after the synthesis.

2.5. MMIPs Characterization

Dynamic light scattering (DLS) was carried out on a Malvern Zetasizer Nano device (Malvern Instruments, Worcestershire, UK) in deionized water (~0.25 mg/mL) at 25 °C.

Transmission electron microscopy (TEM) images were conducted on a Jen-1400 device (Jeol, Tokyo, Japan) at an accelerating voltage of 80 kV. A drop of a sample was allowed to adsorb for 1 min on a copper grid covered with formvar film. The images were captured by a side-mounted Veleta digital camera (EM SIS, Muenster, Germany).

Atomic force microscopy (AFM) was performed using a MultiMode 8™ scanning probe microscope (Bruker, Billerica, MA, USA) connected to a NanoScope® V controller (Veeco, Plainview, NY, USA). The prepared samples were applied in a volume of 7 µL to a freshly pierced 1 × 1 cm² mica surface, washed 3 times after 1 min with 1 mL of MQ water, dried in a stream of argon, and studied by AFM. The surface images were obtained in the ScanAsyst mode of the microscope under atmospheric conditions using a Silicon Tip of Nitride Lever SCANASYST-AIR (Bruker, MA, USA) with the parameters of the radius of curvature of 2 nm, resonance frequency of 45–95 kHz, and force constant of 0.2–0.8 N/m. The obtained images were processed and analyzed using Nanoscope Analysis 1.40 software (Bruker, MA, USA). The dimensional characteristics of the sample in the AFM images were determined using the particle analysis function by analyzing at least three typical images of the same scale from different locations of the mica surface with the applied sample.

FTIR spectra were measured on a 640-IR FT-IR spectrometer (Varian, Peabody, MA, USA) from 4000 to 400 cm⁻¹ at 25 °C accompanied by a KBr pellet.

Electronic absorption spectra were recorded on a UV-2100 spectrometer (Shimadzu, Kyoto, Japan) or microplate reader Clariostar monochromator fluorimeter/luminometer/spectrophotometer (BMG, Ortenberg, Germany).

2.6. Methylene Blue (MB) Capture Analysis for MMIPs and MNIPs

To 10 µL (20 mg/mL) aliquots of MMIPs and MNIPs suspensions, various amounts of MB (0.001–0.04 mg/mL) using 1 mg/mL aqueous stock solution were added. The volume of the reaction mixture was brought to 0.2 mL and incubated for 30 min at 25 °C under stirring (1400 rpm). Afterward, the mixtures were magnetically separated. MB solutions were analyzed by UV-vis at 660 nm on a Clariostar microplate spectrophotometer (BMG, Ortenberg, Germany) at 25 °C in a Costar-96 96-well plate. The amount of MB was calculated using a serial dilution of a dye standard solution.

2.7. Reusability Study of MMIPs

A reusability study of MMIPs was performed for MMIP_0.5, MMIP_2, and MMIP_5 samples. Briefly, 1 mg of MMIP_0.5, MMIP_2, and MMIP_5 was mixed with 0.2 mL of MB (0.02 mg/mL) and incubated for 30 min at 25 °C under stirring (1400 rpm), followed by supernatant analysis by UV at 660 nm. Afterward, MMIPs were magnetically separated, and the solution was removed. To extract MB from the polymer structure, MMIPs were incubated with an aqueous solution containing 1% glacial acetic acid and 1% SDS at 60 °C for 1 h under stirring (1400 rpm), magnetically separated, and washed twice with water. Adsorption/desorption of the MB cycle was repeated at least 4 times.

2.8. Selectivity Study of MMIPs with MB, Toluidine Blue (TB), and Hydroxyethylphenazine (PH)

To 10 μL (20 mg/mL) aliquots of MMIPs and MNIPs suspensions, various amounts of MB, TB, or PH dyes using 1 mg/mL aqueous stock solution were added. The volume of the reaction mixture was brought to 0.2 mL and incubated for 12 h at 25 $^{\circ}\text{C}$ under stirring (1400 rpm). Afterward, the mixtures were magnetically separated. The concentration of free dyes was determined by UV-vis at 660 nm (MB), 620 nm (TB), and 390 nm (PH). The amount of dye was calculated using a serial dilution of a dye standard solution.

2.9. MB Capture by MMIPs from the Lake Water MB Solution

To 1.5 mg of MMIP_2, 0.3 mL of MB solution in Novosibirsk city lake water (0.02 mg/mL) was added and incubated for 30 min at 25 $^{\circ}\text{C}$ under stirring (1400 rpm) followed by supernatant analysis by UV at 660 nm.

3. Results and Discussion

3.1. Synthesis of Magnetic Imprinted Polymers (MMIPs) and Magnetic Nonimprinted Polymers (MNIPs)

In the present work, we used the off-the-shelf polymer method (Figure 1) to produce nylon-based MMIPs [10]. Methylene blue (MB) was chosen as a model pollutant for magnetic separation applications, showing the possibility of MMIP synthesis and essential characteristics of imprinting properties. A schematic representation of the MMIP synthesis scheme is presented in Figures 2 and 3. A 2,2,2-trifluoroethanol (TFE) solvent provides a high solubility for nylon-6 and is capable of mixing with water in any ratio. Previously, in our laboratory [39,42], nylon-6 solution in TFE with a concentration of up to 10 mg/mL, containing up to 30% of water, does not exhibit aggregation of nylon chains. By increasing the water content in the mixture, nylon-6 can be transferred from a dissolved to a solid state. The presence of water in the polymer solution makes it possible to add water-soluble components to the mixture, which can be used as a potential template for molecular imprinting.

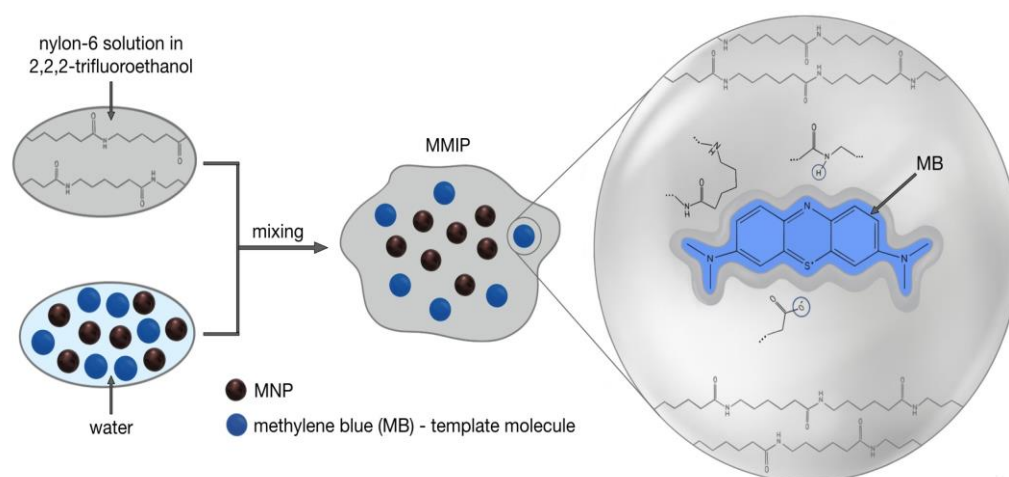


Figure 2. Schematic representation of MMIP synthesis.

To optimize the composition of the MMIPs, the amount of the magnetic core was varied from 0.5 to 5 mg per synthesis (Figure 4, Table 1). With an increase in MNP content, the size of the MMIPs increased from 66.7 nm to 173.8 nm by dynamic light scattering (DLS) (Table 1). MNIPs were also prepared as a control from the same initial solutions and magnetite amount without an MB template. A similar trend of increasing size was also observed for MNIPs.

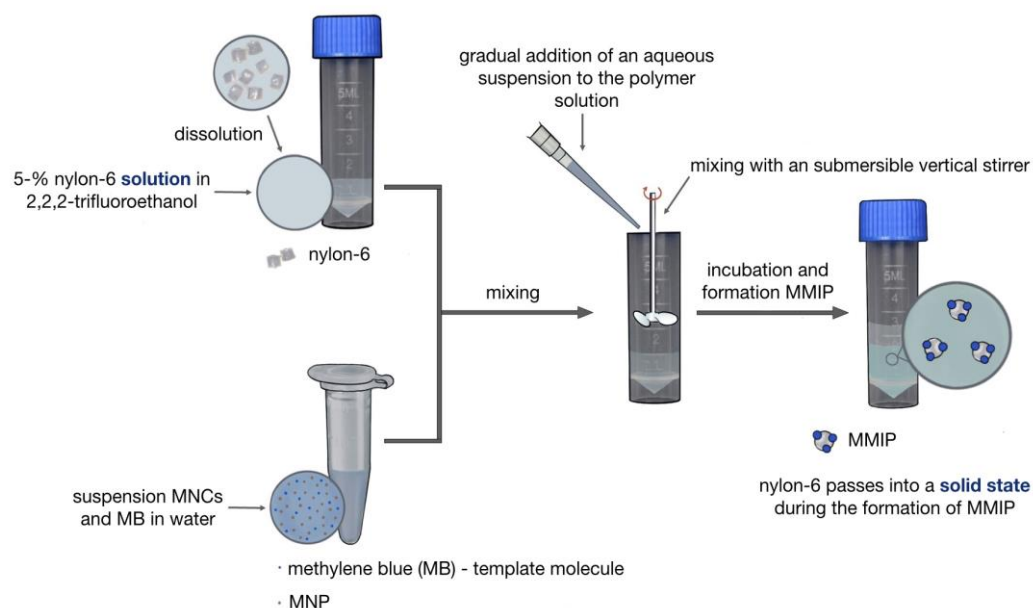


Figure 3. MMIP manufacturing scheme. To synthesize MMIPs, we dissolved nylon-6 in TFE and mixed it with MB and MNPs aqueous solution. To extract the template molecules from the polymer structure, MMIPs were incubated with the aqueous solution containing 5% glacial acetic acid and 5% sodium dodecyl sulfate.

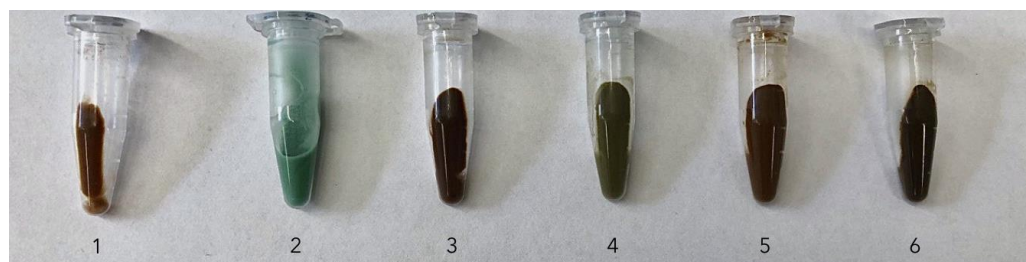


Figure 4. MMIP and MNIP images before MB removal with different amounts of MNPs: 0.5 mg (MNIP_0.5 (1), MMIP_0.5 (2)); 2 mg (MNIP_2 (3), MMIP_2 (4)); 5 mg (MNIP_5 (5), MMIP_5 (6)).

Table 1. The size of MMIPs and MNIPs was estimated using DLS.

Sample Name	MNPs Amount for Synthesis	Hydrodynamic Diameter, nm
MMIP_0.5	0.5 mg	66.7 ± 10.2
MMIP_2	2 mg	103.1 ± 24.6
MMIP_5	5 mg	173.8 ± 24.5
MNIP_0.5	0.5 mg	86.9 ± 29.1
MNIP_2	2 mg	105.0 ± 17.2
MNIP_5	5 mg	144.1 ± 23.3

The morphologies of the obtained MMIPs were characterized via transmission electron microscopy (TEM) (Figure 5). Small-sized MNPs (~13 nm) were wrapped by nylon forming high-sized MMIPs with a branched rich three-dimensional structure and a diameter of 200–500 nm. The broad size distribution of MMIP particles may be attributed to the uneven stirring speed during nylon precipitation. The difference in MNP content was easily visualized by TEM (cf. MMIP_0.5 and MMIP_5). MMIP_5 contained many inclusions of MNPs that principally form cluster-like agglomerates on the surface of nylon [39]. For MMIP_0.5 and MMIP_2, MNPs were located in the bulk of the polymer (Figure 5).

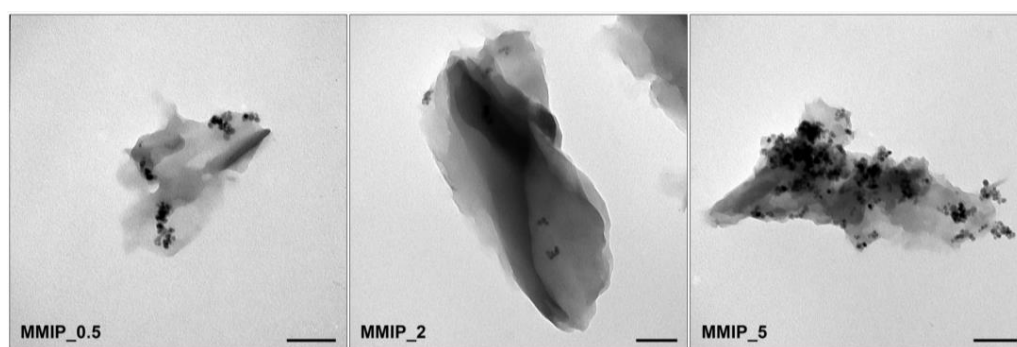


Figure 5. TEM images of MMIP_0.5, MMIP_2, and MMIP_5. The bar indicates 100 nm.

When studied by atomic force microscopy (AFM) (Figure 6A), the MMIP_0.5 sample at a concentration of 142 μM was visualized on the surface as irregularly shaped clusters, among which three different populations could be distinguished according to their size characteristics. For MMIP_0.5, the largest group (450 particles) was represented as 19.2 ± 7.0 nm, the second population (50 particles) showed formations with a diameter of 46.0 ± 5.9 nm, and the third population (16 particles) was 73.4 ± 9.2 nm. A similar trend was obtained for MMIP_2 (Figure 6B). The largest part of the particles (498 particles) were small-sized, with a diameter of 17.7 ± 5.2 nm. Moreover, nanoparticles with a diameter of 40.8 ± 4.8 nm (85 particles) and 60.8 ± 6.5 nm (17 particles) were obtained. Unfortunately, AFM data for MMIP_5 could not be received.

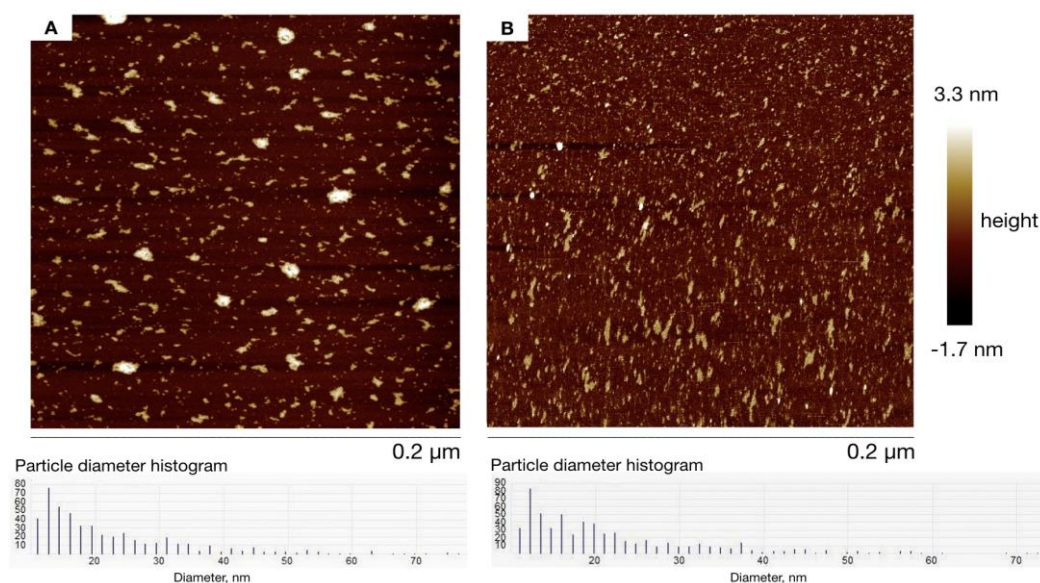


Figure 6. AFM image of MMIP_0.5 (A) and MMIP_2 (B) with a size distribution diagram.

To confirm the components of MMIPs, the Fe_3O_4 nanoparticles (MNP), MNIP_5, and MMIP_5 complex with MB FTIR spectra were recorded (Figure 7). The FTIR spectrum of MNP provides the characteristic peaks of the magnetic core at 580 cm^{-1} (Fe-O stretch), and OH stretching at 1625 cm^{-1} and 3419 cm^{-1} [53–56]. MNIP and MMIP had almost the same FTIR spectrum due to the same nylon-6 and MNP nature (Figure 7). The characteristic peaks were found at 1260 (C-N, N-H), 1382 (CH_2 wagging), 1550 (C-N, N-H), 1652 (amide C=O stretch), 2869 (CH_2 symmetric stretch), 2936 (CH_2 asymmetric stretch), 3307 (N-H stretch), and 3440 cm^{-1} (O-H and N-H stretch) [43,57–59], which shows a good correlation with nylon-6 polymer (see <https://spectra.chem.ut.ee/textile-fibres/polyamide/>, accessed on 28 June 2023). Moreover, broad peaks at $580\text{--}700\text{ cm}^{-1}$ corresponded to a combination

of nylon and magnetite stretches. It is not possible to distinguish MB peaks by FTIR due to the low amount of MB in complexes with MMIPs.

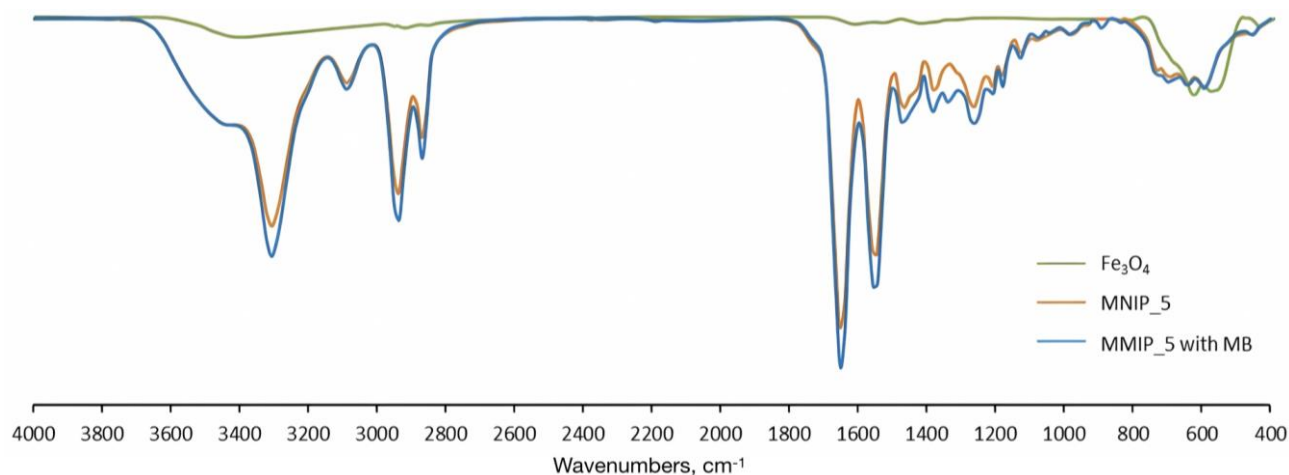


Figure 7. FTIR spectra of MNP, MNIP_5, and MMIP_5 complex with MB.

The various stages of the MMIP preparation were analyzed by UV-vis spectroscopy. It was shown that after the MB was completely removed from the MMIP by careful washing, a TFE solution of MMIPs showed no absorption at 660 nm (Figure 8). On the contrary, the MB and MMIP complex showed a maximum at 660 nm, which may be assigned to MB. It should be noted that in the TFE solution, MB had only one pronounced peak with a maximum of 660 nm. The MMIP_0.5, MMIP_2, and MMIP_5 samples had enough magnetic properties for the magnetic separation procedure (Figure 9). MMIP_5 and MMIP_0.5 magnetically separated for 10 s and 3 min, respectively, which can be explained by the lower MNP amount in MMIP_0.5.

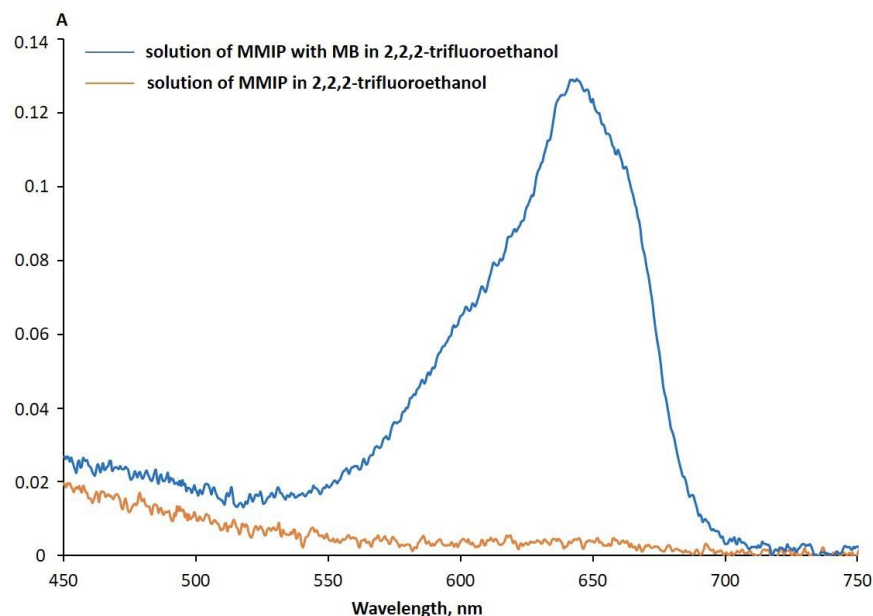


Figure 8. UV-vis spectra of MMIP_5 in TFE and MMIP_5 and MB complex in TFE.

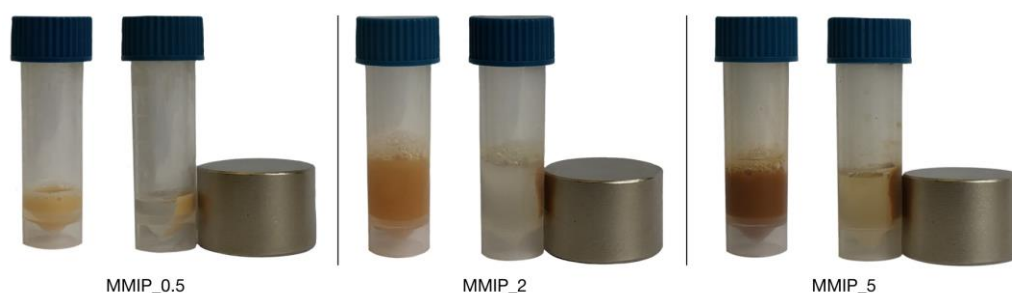


Figure 9. MMIP_0.5, MMIP_2, and MMIP_5 without (left) and with (right) magnet.

3.2. MB Capture by MMIPs and MNIPs

After washing, both MNIPs and MMIPs were incubated with aqueous solutions of MB. The binding experiments were performed at various MB concentrations in the range of 3–125 μM . Afterwards, the absorption at 660 nm was registered. Adsorption capacity (Q_c) is an important indicator for characterizing MIPs. The effect of initial MB concentration on the Q_c parameter was evaluated. The equilibrium adsorbing quantity for MB Q_c can be calculated from the following equation: Q_c ($\mu\text{mol/g}$) = $(C_0 - C_e) \times V/W$, where C_0 (μM) and C_e (μM) are the MB concentrations before and after binding, respectively, V (L) is the volume of MB solution, and W (g) is the mass of the sample. Despite the fact that adsorption kinetics is a very important factor affecting assay performance, the adsorption for all MMIP samples reached adsorption equilibrium for 1–3 min. Therefore, it is quite difficult to analyze the rate of the adsorption quantitatively and calculate the rate constant. These results indicate that MMIPs exhibit a good imprinting effect. The Q_c of MMIPs due to imprinting cavities and the specific adsorption sites were always higher than for MNIPs and increased with the concentration (Figure 10).

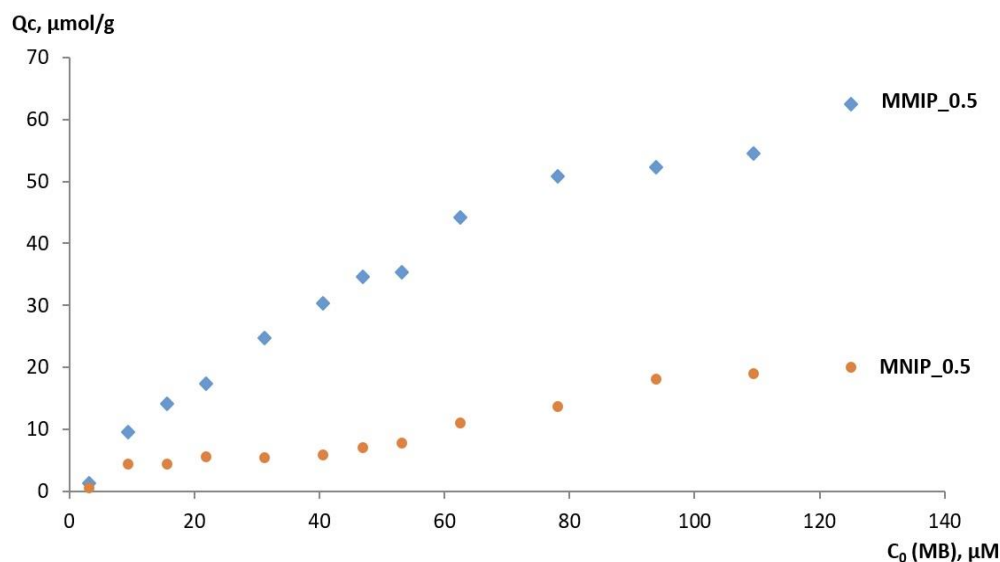


Figure 10. The relationship between adsorbing capacity Q_c and the initial concentration (C_0) of MB for MMIP_0.5 and MNIP_0.5.

The adsorption of MB by MNIPs mainly depended on nonspecific adsorption on the surface of MNIPs. The MB molecules could quickly enter into the imprinted cavities on the surface of MMIPs and were retained in the cavities stably through the formation of hydrogen bonds and hydrophobic and electrostatic interactions (Figure 2). MMIPs contain imprints that allow specific recognition of the MB in the solution. The maximum Q_c of the MMIPs for MB reached 62.4 $\mu\text{mol/g}$ and 110 $\mu\text{mol/g}$ for MMIP_0.5 and MMIP_5, respectively. The low Q_c of MNIPs may be attributed to the absence of proper cavities

and recognition sites, which corresponds to a non-specific process. Molecular recognition selectivity can be evaluated with the specificity coefficient (C_s), which is the ratio of efficiencies of MMIP-template to MNIP-template binding. The C_s values of 4.9 ± 0.3 , 4.2 ± 0.8 , and 5.4 ± 0.2 for $62.5 \mu\text{M}$ MB were obtained for MMIP_0.5, MMIP_2, and MMIP_5, respectively. MMIPs possessed a high adsorption capacity in the range of 20.0–34.8 mg/g with good imprinting factors ranging from 4.2 to 5.4. The presented data are comparable to MMIPs obtained with standard polymerization technology [24]. These results confirm the recognition ability of MMIPs, which was 4–5-fold higher than for the MNIPs.

The affinity of MMIPs and MNIPs to MB was analyzed as described earlier [37] using Scatchard analysis: $\text{MB}(\text{bound})/[\text{MB}(\text{free})] = (\text{PS} - \text{MB}(\text{bound}))/K_d$, where K_d is the equilibrium constant of MB binding to the MMIPs (M), $[\text{MB}(\text{free})]$ is free MB concentration in solution (M), $\text{MB}(\text{bound})$ is the amount of MB subunits bound to the polymer (mol), and PS is the apparent maximum number of the binding sites on the polymer (mol/g per polymer mass). Scatchard plots obtained from the rebinding experiments could be characterized by single straight lines with a good correlation (Figure 11). The calculated K_d values for MMIP_0.5 and MNIP_0.5 were $(2.1 \pm 0.3) \times 10^{-5}$ M and $(3.0 \pm 0.2) \times 10^{-4}$ M, respectively. For MMIP_2 and MMIP_5, K_d values were $(1.2 \pm 0.3) \times 10^{-7}$ M and $(3.1 \pm 0.2) \times 10^{-7}$ M, respectively. Considering the K_d values, MMIPs contained a high-affinity binding site for specifically adsorbing MB, while MNIPs had a negligible affinity binding site for adsorbing MB nonspecifically. These results confirmed that the prepared MMIP showed good binding ability for a studied analyte. The presented data are comparable to MMIPs obtained by standard polymerization technology [60].

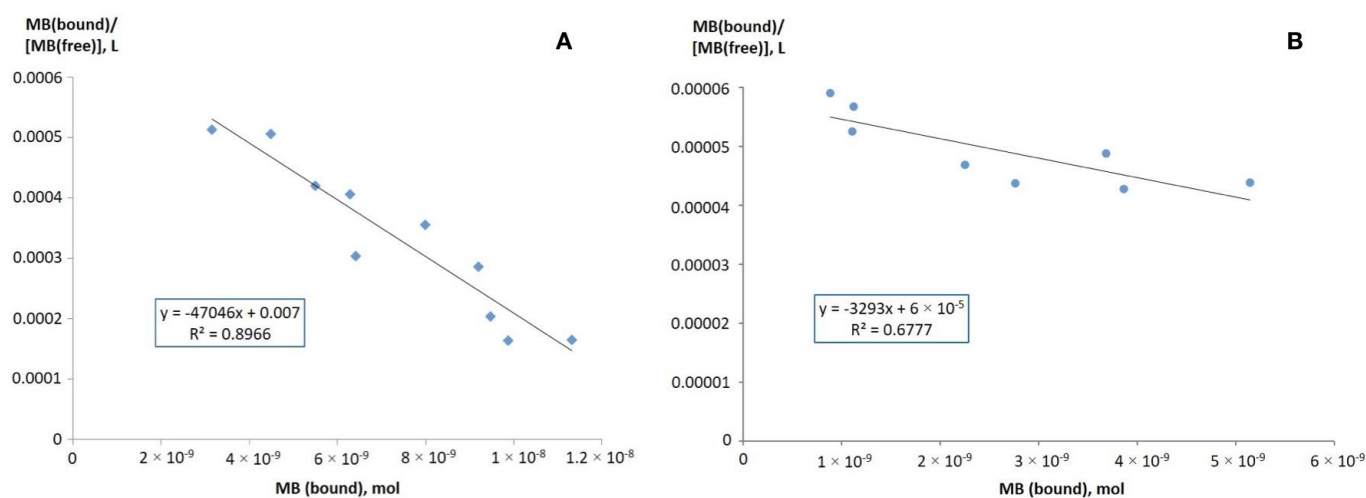


Figure 11. The affinity of MMIP_0.5 (A) and MNIP_0.5 (B) to MB using Scatchard analysis.

3.3. Reusability Study of MMIPs

Reusability provides a great economic benefit and is considered a key factor in the use of materials for solid-phase extraction [60,61]. MMIPs' reusability is much easier than for MIPs due to their magnetic properties. Herein, MMIPs were used for the adsorption of MB in four consecutive adsorption/desorption cycles. The adsorption efficiency for each cycle is shown in Figure 12. The extraction recovery for MMIP_0.5 decreased significantly with an increase in cycle number due to the imprinting sites' destruction during repeated elution. The reusability efficiency of MMIP_0.5 was lower than MMIP_2 and MMIP_5 (Figure 12). This might be attributed to the much lower content of magnetic nanoparticles in MMIP_0.5, which led to the lower recycled amount during the reusability test. A non-significant decrease in MB binding efficiency after each adsorption/desorption cycle was obtained for MMIP_5, which may be attributed to the loss of some binding sites due to comprehensive repeated washing. Moreover, the most decrease in binding efficiency was obtained after the first circle and remained at the same level for four cycles, suggesting that the MMIPs

can even be used during more cycles. MMIP_5 showed outstanding reusability and could be washed and reused without a significant decrease in the binding capacity.

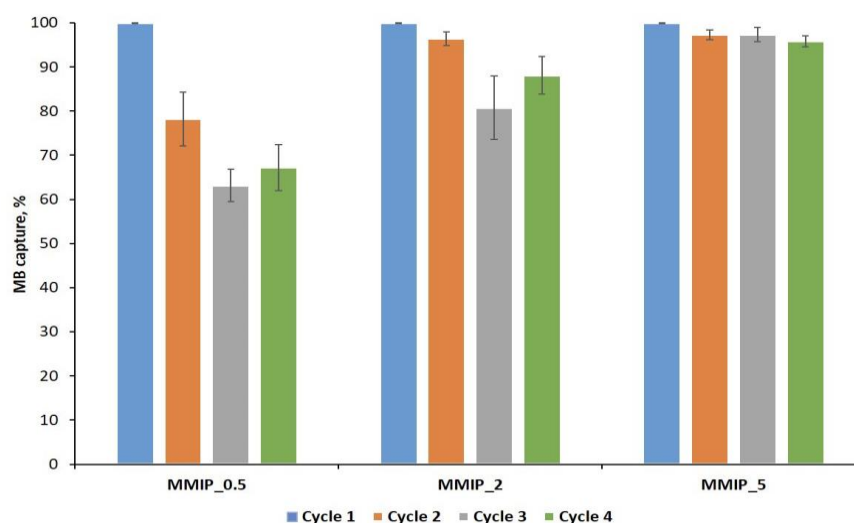


Figure 12. Repeating utilization efficiency of MMIP_0.5, MMIP_2, and MMIP_5.

3.4. Selectivity of MMIP Binding of MB and Its Analogs

To determine the selectivity of MB and its analogs binding to MMIPs, MMIP_0.5, and MNIP_0.5 were studied for MB, hydroxyethylphenazine (PH), and toluidine blue (TB) adsorption. The binding procedure is presented in Figure 13. The amount of dye was analyzed by UV-vis and was calculated using a serial dilution of a dye standard solution.

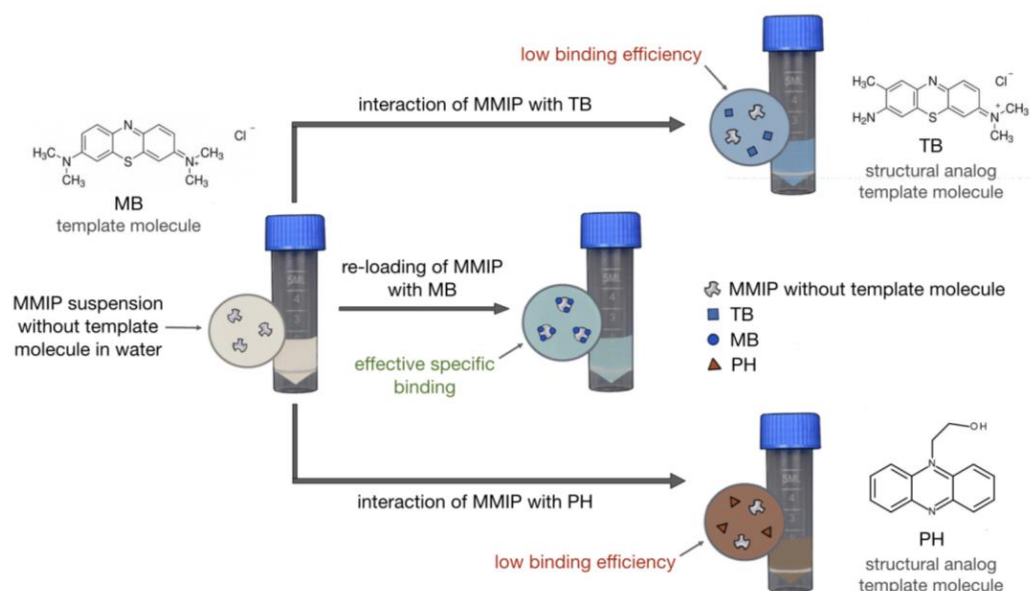


Figure 13. Scheme of dyes binding to the MMIP and MNIP experiment.

Figure 14 shows the Q_c value for various dyes (MB, PH, and TB) depending on dye concentration for MMIP_0.5. It was found that the Q_c of MMIP_0.5 per MB was significantly higher than for PH and TB. Moreover, the Q_c for PH dye was low. Such a difference in Q_c value for PH and TB may be explained by the higher structural similarity of TB to MB.

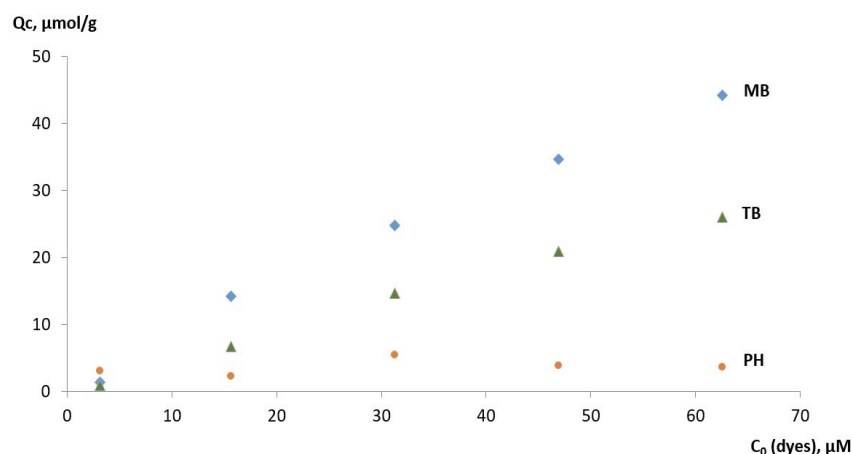


Figure 14. The relationship between Q_c and the initial concentration C_0 of different dyes for MMIP_0.5.

Figure 15 provides the data of Q_c for MMIP_0.5 and MNIP_0.5 and 15 μM dye concentration, which may be attributed to the selectivity parameter. The values of the adsorption selectivity coefficient (S), which is the ratio of efficiencies binding of MMIP_0.5 with MB to PH or TB, respectively, were estimated for all dyes. The S values were calculated at 6.1 ± 0.6 and 2.1 ± 0.3 for PH and TB, respectively, for 15 μM dye concentration. However, the S value increased up to 12, while the PH concentration increased (see Figure 15). The highest Q_c value of MB on MMIPs means that MMIPs had the highest affinity for MB (the template molecule) compared to the other compounds. The analogs had the similarity of functional groups, which can generate hydrogen, electrostatic, and hydrophobic interaction with MMIPs. However, the template molecule (MB) had the highest adsorbed amount because the interaction between the imprinted polymer and the target analyte depends not only on interactions with functional groups, but is also related to the specific cavity memory of the size, shape, and functional group of the template. Therefore, MMIPs demonstrated specific recognition sites for MB extraction. MMIPs have shown a high potential in the specific identification of analytes. Thus, we demonstrated that simple polyamides, such as nylon-6, when structured in the presence of template molecules, acquire a molecular memory and become capable of the specific recognition of a template.

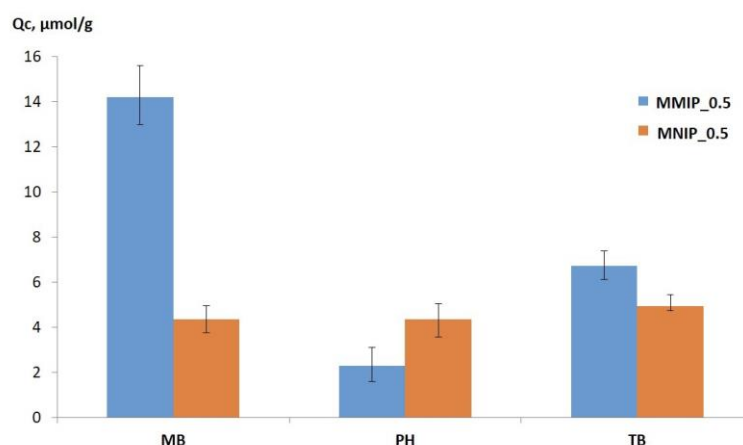


Figure 15. Adsorption selectivity of MMIP_0.5 and MNIP_0.5 to different dyes. The concentration of dyes is 15 μM .

3.5. MMIP Interaction with a Model MB Solution

We have demonstrated that MMIPs can also be effective when interacting with model wastewater samples, mimicking real pollutant situations. For example, we dissolved MB in lake water, which was further used for MB capture. After the addition of MMIPs to

the model sample with MB, the mixture was incubated for 30 min at 25 °C under stirring (1400 rpm) followed by the absorption spectra recording (Figure 16). The efficiency of MB capture of MMIPs was calculated as 91%. Such high extraction efficiency indicates good application prospects for wastewater treatment.

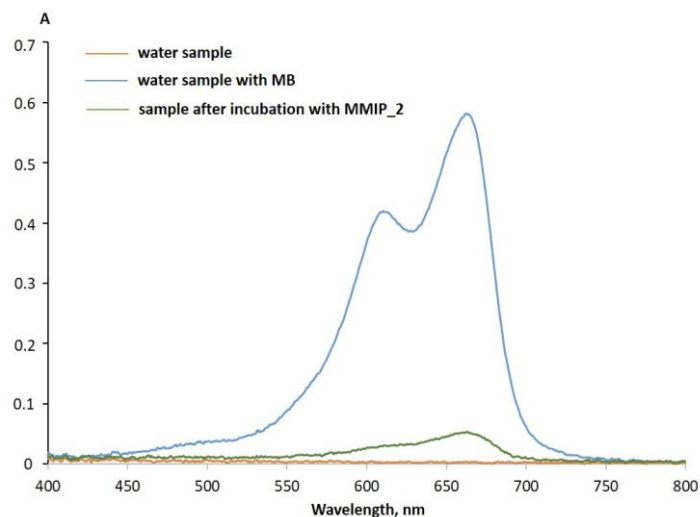


Figure 16. UV spectra of the lake water sample (orange line, control sample), lake water with diluted MB sample (blue line), and the sample after incubation with MMIPs (green line).

4. Conclusions

A novel simple approach for the preparation of nylon-based magnetic imprinting polymers for MB dye capture was developed. The polymer matrix was formed during the transition of off-the-shelf nylon-6 from a dissolved state to a solid state in the presence of template molecules and Fe₃O₄ nanoparticles in the initial solution. To improve the magnetic properties and aggregation ability of MMIPs, the concentration of the magnetic core was varied. By examining the magnetic properties of three MMIP samples, MMIP_5 showed the highest magnetic properties and magnetic separation of template molecules. The material was stable in water solution for not less than half of the year. To serve as a solid-phase magnetic absorbent, MMIPs were studied in terms of adsorbing capacity, affinity, and selectivity of MB and structural analogs (PH and TB). MMIPs possessed a high adsorption capacity in the range of 20.0–34.8 mg/g with good imprinting factors ranging from 4.2 to 5.4. MMIP_5 exhibited the highest adsorption capacity of MB, reaching 110 μmol/g, which was 5.4-fold higher than for the non-imprinted analog. The selectivity coefficients toward MB structural analogs were estimated to be 6.1 ± 0.6 and 2.1 ± 0.3 for 15 μM PH and TB, which shows excellent MMIP selectivity. MMIP_5 provided remarkable reusability on four MB absorption and release cycles, highlighting ~95% extraction efficiency step by step. Based on the established stability, physico-chemical properties, high adsorption, selectivity towards structural analogs, and specificity for the target molecule, the proposed MMIP technology has excellent application prospects in MB-containing wastewater sample recycling. We believe that molecular imprinting technology, as shown in MB magnetic separation example, will bring quality improvements to other template molecules' analysis and the whole research area of MMIPs for various applications. The possibility of using the magnetic properties of MMIPs is an essential feature for industrial manufacturing, sensor application, and mass production.

Author Contributions: Conceptualization, E.D.; methodology, E.D.; investigation, A.S. and E.D.; data curation, Y.P., V.G., A.S. and E.D.; writing—original draft preparation, A.C. and E.D.; project administration, E.D.; funding acquisition, A.C. and E.D. All authors have read and agreed to the published version of the manuscript.

Funding: This study was funded by the Ministry of Science and Higher Education of the Russian Federation (state registration No. 121031300042-1).

Institutional Review Board Statement: Not applicable.

Informed Consent Statement: Not applicable.

Data Availability Statement: Not applicable.

Acknowledgments: We thank Ryabchikova E. I. (ICBFM SB RAS) for fruitful discussion and support with TEM images. We thank Kirillov V.L. (Boreskov Institute of Catalysis SB RAS) for the fruitful discussion concerning MNP synthesis.

Conflicts of Interest: The authors declare no conflict of interest. The funders had no role in the design of the study; in the collection, analyses, or interpretation of data; in the writing of the manuscript; or in the decision to publish the results.

References

1. Khitous, A.; Molinaro, C.; Gree, S.; Haupt, K.; Soppera, O. Plasmon-Induced Photopolymerization of Molecularly Imprinted Polymers for Nanosensor Applications. *Adv. Mater. Interfaces* **2023**, *10*, 2201651. [[CrossRef](#)]
2. Meng, H.; Zhao, T.; Jing, T.; Zeng, Y.; Wang, N. Preparation and Properties of Novel Magnetic Methylene Blue Molecularly Imprinted Polymer. *Polym. Sci. Ser. B* **2021**, *63*, 245–256. [[CrossRef](#)]
3. Zhao, X.; Liu, S.; Tang, Z.; Niu, H.; Cai, Y.; Meng, W.; Wu, F.; Giesy, J.P. Synthesis of Magnetic Metal-Organic Framework (MOF) for Efficient Removal of Organic Dyes from Water. *Sci. Rep.* **2015**, *5*, 11849. [[CrossRef](#)] [[PubMed](#)]
4. Silva, A.L.G.; Carvalho, N.V.; Paterno, L.G.; Moura, L.D.; Filomeno, C.L.; de Paula, E.; B ao, S.N. Methylene Blue Associated with Maghemite Nanoparticles Has Antitumor Activity in Breast and Ovarian Carcinoma Cell Lines. *Cancer Nanotechnol.* **2021**, *12*, 11. [[CrossRef](#)]
5. Khan, I.; Saeed, K.; Zekker, I.; Zhang, B.; Hendi, A.H.; Ahmad, A.; Ahmad, S.; Zada, N.; Ahmad, H.; Shah, L.A.; et al. Review on Methylene Blue: Its Properties, Uses, Toxicity and Photodegradation. *Water* **2022**, *14*, 242. [[CrossRef](#)]
6. Popadi c, D.; Gavrilov, N.; Ignjatovi c, L.; Kraji nik, D.; Mentus, S.; Milojevi c-Raki c, M.; Bajuk-Bogdanovi c, D. How to Obtain Maximum Environmental Applicability from Natural Silicates. *Catalysts* **2022**, *12*, 519. [[CrossRef](#)]
7. Ramin, N.A.; Ramachandran, M.R.; Saleh, N.M.; Mat Ali, Z.M.; Asman, S. Magnetic Nanoparticles Molecularly Imprinted Polymers: A Review. *Curr. Nanosci.* **2022**, *18*, 372–400. [[CrossRef](#)]
8. Meseguer-Lloret, S.; Torres-Cartas, S.; G omez-Benito, C.; Herrero-Mart nez, J.M. Magnetic Molecularly Imprinted Polymer for the Simultaneous Selective Extraction of Phenoxo Acid Herbicides from Environmental Water Samples. *Talanta* **2022**, *239*, 123082. [[CrossRef](#)]
9. Fresco-Cala, B.; Batista, A.D.; C ardenas, S. Molecularly Imprinted Polymer Micro- and Nano-Particles: A Review. *Molecules* **2020**, *25*, 4740. [[CrossRef](#)]
10. Dmitrienko, E.V.; Pyshnaya, I.A.; Martyanov, O.N.; Pyshnyi, D. V Molecularly Imprinted Polymers for Biomedical and Biotechnological Applications. *Russ. Chem. Rev.* **2016**, *85*, 513–536. [[CrossRef](#)]
11. Akg n ll , S.; Kılı , S.; Esen, C.; Denizli, A. Molecularly Imprinted Polymer-Based Sensors for Protein Detection. *Polymers* **2023**, *15*, 629. [[CrossRef](#)] [[PubMed](#)]
12. Ariani, M.D.; Zuhrotun, A.; Manesiotis, P.; Hasanah, A.N. Magnetic Molecularly Imprinted Polymers: An Update on Their Use in the Separation of Active Compounds from Natural Products. *Polymers* **2022**, *14*, 1389. [[CrossRef](#)]
13. Zhang, W.; Li, Q.; Li, J.; Sun, X.; Shen, J.; Han, W.; Wang, L. The Preparation of Layered Hierarchical and Cube-Shaped Magnetic Fe₃O₄/CaCO₃ for Efficient Enrichment of Pb(II) from Aqueous Solutions. *Environ. Nanotechnol. Monit. Manag.* **2021**, *16*, 100600. [[CrossRef](#)]
14. Murdaya, N.; Triadenda, A.L.; Rahayu, D.; Hasanah, A.N. A Review: Using Multiple Templates for Molecular Imprinted Polymer: Is It Good? *Polymers* **2022**, *14*, 4441. [[CrossRef](#)]
15. Huang, X.C.; Ma, J.K.; Wei, S.L. Preparation and Application of a Novel Magnetic Molecularly Imprinted Polymer for Simultaneous and Rapid Determination of Three Trace Endocrine Disrupting Chemicals in Lake Water and Milk Samples. *Anal. Bioanal. Chem.* **2020**, *412*, 1835–1846. [[CrossRef](#)] [[PubMed](#)]
16. Wei, S.L.; Liu, W.T.; Huang, X.C.; Ma, J.K. Preparation and Application of a Magnetic Plasticizer as a Molecularly Imprinted Polymer Adsorbing Material for the Determination of Phthalic Acid Esters in Aqueous Samples. *J. Sep. Sci.* **2018**, *41*, 3806–3814. [[CrossRef](#)]
17. Ma, J.K.; Huang, X.C.; Wei, S.L. Rapid Determination of Antiviral Medication Ribavirin in Different Feedstuffs Using a Novel Magnetic Molecularly Imprinted Polymer Coupled with High-Performance Liquid Chromatography. *J. Sep. Sci.* **2019**, *42*, 3372–3381. [[CrossRef](#)]
18. Li, J.; Wang, Y.; Yu, X. Magnetic Molecularly Imprinted Polymers: Synthesis and Applications in the Selective Extraction of Antibiotics. *Front. Chem.* **2021**, *9*, 706311. [[CrossRef](#)]

19. Lazar, M.M.; Ghiorghita, C.A.; Dragan, E.S.; Humelnicu, D.; Dinu, M.V. Ion-Imprinted Polymeric Materials for Selective Adsorption of Heavy Metal Ions from Aqueous Solution. *Molecules* **2023**, *28*, 2798. [[CrossRef](#)]
20. Zhao, G.; Zhang, Y.; Sun, D.; Yan, S.; Wen, Y.; Wang, Y.; Li, G.; Liu, H.; Li, J.; Song, Z. Recent Advances in Molecularly Imprinted Polymers for Antibiotic Analysis. *Molecules* **2023**, *28*, 335. [[CrossRef](#)]
21. Li, J.; Zhou, Q.; Yuan, Y.; Wu, Y. Iron-Based Magnetic Molecular Imprinted Polymers and Their Application in Removal and Determination of Di-n-Pentyl Phthalate in Aqueous Media. *R. Soc. Open Sci.* **2017**, *4*, 170672. [[CrossRef](#)] [[PubMed](#)]
22. Urriza-Arsuaga, I.; Guadaño-Sánchez, M.; Urraca, J.L. Current Trends in Molecular Imprinting: Strategies, Applications and Determination of Target Molecules in Spain. *Int. J. Mol. Sci.* **2023**, *24*, 1915. [[CrossRef](#)] [[PubMed](#)]
23. Poonia, K.; Raizada, P.; Singh, A.; Verma, N.; Ahamad, T.; Alshehri, S.M.; Khan, A.A.P.; Singh, P.; Hussain, C.M. Magnetic Molecularly Imprinted Polymer Photocatalysts: Synthesis, Applications and Future Perspective. *J. Ind. Eng. Chem.* **2022**, *113*, 1–14. [[CrossRef](#)]
24. Wei, S.; Li, J.; Liu, Y.; Ma, J. Development of Magnetic Molecularly Imprinted Polymers with Double Templates for the Rapid and Selective Determination of Amphenicol Antibiotics in Water, Blood, and Egg Samples. *J. Chromatogr. A* **2016**, *1473*, 19–27. [[CrossRef](#)] [[PubMed](#)]
25. Goyal, G.; Bhakta, S.; Mishra, P. Surface Molecularly Imprinted Biomimetic Magnetic Nanoparticles for Enantioseparation. *ACS Appl. Nano Mater.* **2019**, *2*, 6747–6756. [[CrossRef](#)]
26. Dinc, M.; Esen, C.; Mizaikoff, B. Recent Advances on Core–Shell Magnetic Molecularly Imprinted Polymers for Biomacromolecules. *Trends Anal. Chem.* **2019**, *114*, 202–217. [[CrossRef](#)]
27. Dai, Q.; Wang, Y.; Xu, W.; Liu, Y.; Zhou, Y. Adsorption and Specific Recognition of DNA by Using Imprinted Polymer Layers Grafted onto Ionic Liquid Functionalized Magnetic Microspheres. *Microchim. Acta* **2017**, *184*, 4433–4441. [[CrossRef](#)]
28. Popova, V.; Dmitrienko, E.; Chubarov, A. Magnetic Nanocomposites and Imprinted Polymers for Biomedical Applications of Nucleic Acids. *Magnetochemistry* **2023**, *9*, 12. [[CrossRef](#)]
29. Petrov, K.D.; Chubarov, A.S. Magnetite Nanoparticles for Biomedical Applications. *Encyclopedia* **2022**, *2*, 1811–1828. [[CrossRef](#)]
30. Bobrikova, E.; Chubarov, A.; Dmitrienko, E. The Effect of PH and Buffer on Oligonucleotide Affinity for Iron Oxide Nanoparticles. *Magnetochemistry* **2021**, *7*, 128. [[CrossRef](#)]
31. Pilvenyte, G.; Ratautaite, V.; Boguzaitė, R.; Ramanavicius, A.; Viter, R.; Ramanavicius, S. Molecularly Imprinted Polymers for the Determination of Cancer Biomarkers. *Int. J. Mol. Sci.* **2023**, *24*, 4105. [[CrossRef](#)]
32. Zhang, Y.; Wang, Q.; Zhao, X.; Ma, Y.; Zhang, H.; Pan, G. Molecularly Imprinted Nanomaterials with Stimuli Responsiveness for Applications in Biomedicine. *Molecules* **2023**, *28*, 918. [[CrossRef](#)]
33. Gagliardi, M. Design and Development of Molecularly Imprinted Biodegradable Polymers for Nanomedicine. *Adv. Ind. Eng. Polym. Res.* **2023**. [[CrossRef](#)]
34. Balcer, E.; Sobiech, M. Molecularly Imprinted Carriers for Diagnostics and Therapy—A Critical Appraisal. *Pharmaceutics* **2023**, *15*, 1647. [[CrossRef](#)]
35. Garnier, M.; Sabbah, M.; Ménager, C.; Griffete, N. Hybrid Molecularly Imprinted Polymers: The Future of Nanomedicine? *Nanomaterials* **2021**, *11*, 3091. [[CrossRef](#)]
36. Sanadgol, N.; Wackerlig, J. Developments of Smart Drug-Delivery Systems Based on Magnetic Molecularly Imprinted Polymers for Targeted Cancer Therapy: A Short Review. *Pharmaceutics* **2020**, *12*, 831. [[CrossRef](#)] [[PubMed](#)]
37. Dmitrienko, E.V.; Bulushev, R.D.; Haupt, K.; Kosolobov, S.S.; Latyshev, A.V.; Pyshnaya, I.A.; Pyshnyi, D.V. A Simple Approach to Prepare Molecularly Imprinted Polymers from Nylon-6. *J. Mol. Recognit.* **2013**, *26*, 368–375. [[CrossRef](#)] [[PubMed](#)]
38. Shakiba, M.; Rezvani Ghomi, E.; Khosravi, F.; Jouybar, S.; Bigham, A.; Zare, M.; Abdouss, M.; Moaref, R.; Ramakrishna, S. Nylon—A Material Introduction and Overview for Biomedical Applications. *Polym. Adv. Technol.* **2021**, *32*, 3368–3383. [[CrossRef](#)]
39. Bulgakova, A.; Chubarov, A.; Dmitrienko, E. Magnetic Nylon 6 Nanocomposites for the Microextraction of Nucleic Acids from Biological Samples. *Magnetochemistry* **2022**, *8*, 85. [[CrossRef](#)]
40. Reyes-Gallardo, E.M.; Lucena, R.; Cárdenas, S. Silica Nanoparticles-Nylon 6 Composites: Synthesis, Characterization and Potential Use as Sorbent. *RSC Adv.* **2017**, *7*, 2308–2314. [[CrossRef](#)]
41. Mahfuz, H.; Hasan, M.; Dhanak, V.; Beamson, G.; Stewart, J.; Rangari, V.; Wei, X.; Khabashesku, V.; Jeelani, S. Reinforcement of Nylon 6 with Functionalized Silica Nanoparticles for Enhanced Tensile Strength and Modulus. *Nanotechnology* **2008**, *19*, 445702. [[CrossRef](#)]
42. Popova, V.; Poletaeva, Y.; Chubarov, A.; Pyshnyi, D.; Dmitrienko, E. Doxorubicin-Loaded Silica Nanocomposites for Cancer Treatment. *Coatings* **2023**, *13*, 324. [[CrossRef](#)]
43. Kovrigina, E.; Poletaeva, Y.; Zheng, Y.; Chubarov, A. Nylon-6-Coated Doxorubicin-Loaded Magnetic Nanoparticles and Nanocapsules for Cancer Treatment. *Magnetochemistry* **2023**, *9*, 106. [[CrossRef](#)]
44. Yang, F.; Fu, D.; Li, P.; Sui, X.; Xie, Y.; Chi, J.; Liu, J.; Huang, B. Magnetic Molecularly Imprinted Polymers for the Separation and Enrichment of Cannabidiol from Hemp Leaf Samples. *ACS Omega* **2022**, *8*, 1240–1248. [[CrossRef](#)] [[PubMed](#)]
45. Chubarov, A.S. Serum Albumin for Magnetic Nanoparticles Coating. *Magnetochemistry* **2022**, *8*, 13. [[CrossRef](#)]
46. Mittal, A.; Roy, I.; Gandhi, S. Magnetic Nanoparticles: An Overview for Biomedical Applications. *Magnetochemistry* **2022**, *8*, 107. [[CrossRef](#)]
47. Shabatina, T.I.; Vernaya, O.I.; Shabatin, V.P.; Melnikov, M.Y. Magnetic Nanoparticles for Biomedical Purposes: Modern Trends and Prospects. *Magnetochemistry* **2020**, *6*, 30. [[CrossRef](#)]

48. Socoliuc, V.; Peddis, D.; Petrenko, V.I.; Avdeev, M.V.; Susan-Resiga, D.; Szabó, T.; Turcu, R.; Tombácz, E.; Vékás, L. Magnetic Nanoparticle Systems for Nanomedicine—A Materials Science Perspective. *Magnetochemistry* **2020**, *6*, 2. [[CrossRef](#)]
49. Hepel, M. Magnetic Nanoparticles for Nanomedicine. *Magnetochemistry* **2020**, *6*, 3. [[CrossRef](#)]
50. Niu, M.; Pham-Huy, C.; He, H. Core-Shell Nanoparticles Coated with Molecularly Imprinted Polymers: A Review. *Microchim. Acta* **2016**, *183*, 2677–2695. [[CrossRef](#)]
51. Kirillov, V.L.; Balaev, D.A.; Semenov, S.V.; Shaikhutdinov, K.A.; Martyanov, O.N. Size Control in the Formation of Magnetite Nanoparticles in the Presence of Citrate Ions. *Mater. Chem. Phys.* **2014**, *145*, 75–81. [[CrossRef](#)]
52. Kirillov, V.L.; Yakushkin, S.S.; Balaev, D.A.; Dubrovskiy, A.A.; Semenov, S.V.; Knyazev, Y.V.; Bayukov, O.A.; Velikanov, D.A.; Yatsenko, D.A.; Martyanov, O.N. Dimethylsulfoxide as a Media for One-Stage Synthesis of the Fe₃O₄ -Based Ferro Fluids with a Controllable Size Distribution. *Mater. Chem. Phys.* **2019**, *225*, 292–297. [[CrossRef](#)]
53. Ibarra, J.; Melendres, J.; Almada, M.; Burboa, M.G.; Taboada, P.; Juárez, J.; Valdez, M.A. Synthesis and Characterization of Magnetite/PLGA/Chitosan Nanoparticles. *Mater. Res. Express* **2015**, *2*, 95010. [[CrossRef](#)]
54. Popova, V.; Poletaeva, Y.; Chubarov, A.; Dmitrienko, E. PH-Responsible Doxorubicin-Loaded Fe₃O₄@CaCO₃ Nanocomposites for Cancer Treatment. *Pharmaceutics* **2023**, *15*, 771. [[CrossRef](#)] [[PubMed](#)]
55. Kowalik, P.; Elbaum, D.; Mikulski, J.; Fronc, K.; Kamińska, I.; Morais, P.C.; Eduardo De Souza, P.; Nunes, R.B.; Veiga-Souza, F.H.; Gruzel, G.; et al. Upconversion Fluorescence Imaging of HeLa Cells Using ROS Generating SiO₂-Coated Lanthanide-Doped NaYF₄ Nanoconstructs. *RSC Adv.* **2017**, *7*, 30262–30273. [[CrossRef](#)]
56. Stoia, M.; Istrate, R.; Păcurariu, C. Investigation of Magnetite Nanoparticles Stability in Air by Thermal Analysis and FTIR Spectroscopy. *J. Therm. Anal. Calorim.* **2016**, *125*, 1185–1198. [[CrossRef](#)]
57. Vasanthan, N. Crystallinity Determination of Nylon 66 by Density Measurement and Fourier Transform Infrared (FTIR) Spectroscopy. *J. Chem. Educ.* **2012**, *89*, 387–390. [[CrossRef](#)]
58. Mahdi, H.A. An FTIR Study of Characterization of Neat and UV Stabilized Nylon 6,6 Polymer Films. *J. Pure Appl. Sci.* **2011**, *24*, 86–90.
59. Khor, N.K.E.M.; Salmiati; Hadibarata, T.; Yusop, Z. A Combination of Waste Biomass Activated Carbon and Nylon Nanofiber for Removal of Triclosan from Aqueous Solutions. *J. Environ. Treat. Tech.* **2020**, *8*, 1036–1045. [[CrossRef](#)]
60. Gao, R.; Hao, Y.; Zhao, S.; Zhang, L.; Cui, X.; Liu, D.; Tang, Y.; Zheng, Y. Novel Magnetic Multi-Template Molecularly Imprinted Polymers for Specific Separation and Determination of Three Endocrine Disrupting Compounds Simultaneously in Environmental Water Samples. *RSC Adv.* **2014**, *4*, 56798–56808. [[CrossRef](#)]
61. Ansari, S.; Karimi, M. Recent Configurations and Progressive Uses of Magnetic Molecularly Imprinted Polymers for Drug Analysis. *Talanta* **2017**, *167*, 470–485. [[CrossRef](#)] [[PubMed](#)]

Disclaimer/Publisher's Note: The statements, opinions and data contained in all publications are solely those of the individual author(s) and contributor(s) and not of MDPI and/or the editor(s). MDPI and/or the editor(s) disclaim responsibility for any injury to people or property resulting from any ideas, methods, instructions or products referred to in the content.